Origin of the emergent fragile-to-strong transition in supercooled water

Rui Shi[a], **John Russo**[a,b], **and Hajime Tanaka**[a,1]

[a]Institute of Industrial Science, University of Tokyo, 4-6-1 Komaba, Meguro-ku, Tokyo 153-8505, Japan; [b]School of Mathematics, University of Bristol, Bristol BS8 1TW, United Kingdom

This manuscript was compiled on June 29, 2018

Liquids can be broadly classified into two categories, fragile and strong ones, depending on how their dynamical properties change with temperature. The dynamics of a strong liquid obeys the Arrhenius law, whereas the fragile one displays a super-Arrhenius law, with a much steeper slowing down upon cooling. Recently, however, it was discovered that many materials such as water, oxides, and metals do not obey this simple classification, apparently exhibiting a fragile-to-strong transition far above T_g. Such a transition is particularly well-known for water, and it is now regarded as one of water's most important anomalies. This phenomenon has been attributed to either an unusual glass transition behavior, or to the crossing of a Widom line emanating from a liquid-liquid critical point. Here by computer simulations of two popular water models and through analyses of experimental data, we show that the emergent fragile-to-strong transition is actually a crossover between two Arrhenius regimes with different activation energies, which can be naturally explained by a two-state description of the dynamics. Our finding provides a new insight into the fragile-to-strong transition observed in a wide class of materials.

water's anomalies | structural origin | two-state model | fragile-to-strong transition

A fragile-to-strong transition, or a dynamic crossover from fragile to strong behavior, has attracted considerable attention in water and glass science community. Historically, the first example of such a transition was discovered in a supercooled state of water (1, 2). Although direct observation of such a transition in bulk water was preempted by ice crystallization, many pieces of evidence have been accumulated in confined (3, 4), low-density amorphous (5, 6), high-density amorphous (6) and vapor-deposited amorphous water (5), which consistently shows Arrhenius behavior of water near T_g. These observations, albeit indirectly, strongly support the existence of a fragile-to-strong transition in deeply supercooled water.

Several scenarios have been proposed to account for this transition. We mention here the three most relevant ones for our discussion. The first one was proposed by Angell and coworkers (1, 2, 7), on the basis of experimental observations showing that water is fragile above the homogeneous nucleation temperature T_H, while strong near the glass transition temperature T_g. It ascribes water's dynamic crossover to the glass transition, based either on mode-coupling theory (8) or Adam-Gibbs theory (2, 7). However, this scenario does not explain why the dynamical slowing down appears at a temperature much higher than the glass transition temperature $T_g \sim 136$ K (9). This limitation was circumvented by the introduction of the Widom line (T_W) by Stanley and his coworkers (10). The Widom line is the name given to a family of lines emanating from the liquid-liquid critical point (11, 12) where thermodynamic susceptibilities are maximazed (10). This scenario explains the dynamic anomalies with a crossover from the power-law behavior of high-density liquid water, to the Arrhenius behavior of low-density liquid water at the Widom line. Finally, a two-state scenario was proposed by Tanaka (13, 14) on the basis of the existence of two types of local structures (two states) in liquid water, which interprets the fragile-to-strong transition as a dynamic crossover from the high-temperature disordered state to the low-temperature ordered state, via a mixed state of the two. The advantages of the two-state description is that (i) it can explain both thermodynamic and dynamic anomalies in the same framework and (ii) it provides an account of water anomalies that does not hinge on the power-law divergences of the glass-transition or the second critical point, while still being able to accommodate them.

The fragile-to-strong transition provides a comprehensive description of water's dynamic anomalies, but its physical origin remains elusive. This is because all three scenarios provide a reasonably good description above T_W, and predict different behavior only below T_W. New measurements and simulations in this deeply supercooled regime are thus needed to understand the nature of the fragile-to-strong transition in liquid water.

Great progress on the detection of liquid water in deeply supercooled regime has been made recently. For example, the maximum of isothermal compressibility, known as the Widom line, has been observed at 229.2 K in water droplets by femtosecond x-ray scattering (15). Moreover, the diffusion

Significance Statement

Upon cooling, the liquid dynamics generally slows down, with a rate that either keeps constant for a strong liquid, or monotonically increases for a fragile one. However, water, silica, and some metallic liquids do not obey this general rule and the rate exhibits a maximum. This unusual phenomenon is known as the fragile-to-strong transition and its origin remains very controversial. Here we show that the fragility of water is only apparent, and that it originates from crossover between a high-temperature liquid without locally favored structures, and a low-temperature one full of them, both of which have Arrhenius dynamics. Given its generality, this explanation of dynamic anomalies may be common to any liquids having a tendency to form locally favored structures.

H.T. proposed and supervised the study, R.S. performed numerical simulations and analysis, all authors discussed the results and wrote the manuscript.

The authors declare no conflict of interest.

[1]To whom correspondence should be addressed. E-mail: tanaka@iis.u-tokyo.ac.jp

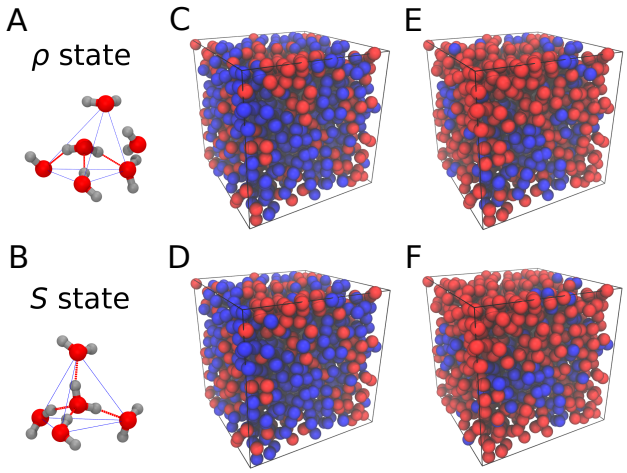

Fig. 1. Water's local structures and their correlations to local density and mobility. (A)-(B) Typical snapshots of water's local structures for ρ and S states. The dot red lines represent H-bonds and the solid blue lines show the tetrahedral structure. (C)-(F) Different fields for a sample configuration for the TIP5P water at 0.1 MPa and 250 K. All molecules (only oxygen atoms are shown) are colored in red if the field is low, or blue if it is high. (C) ζ field. (D) Inverse local density field ($6 - N_{\rm fs}$, where $N_{\rm fs}$ is the number of first-shell neighbors). (E) $\zeta^{\rm CG}$ field. (F) Inverse mobility field ($1 - \Delta r_{\rm max}(\tau_4)$), where $\Delta r_{\rm max}(\tau_4)$ is the maximum distance one molecule traveling during a time period of τ_4 (τ_4: dynamic heterogeneity time scale. See SI Secs. VI and VII). In (C)-(E) a simple low-pass filter by performing rolling time average of each field over τ_4 is used to remove thermal fluctuations. In (C)-(D) and (E)-(F), 58% and 26% molecules with higher field are colored in blue, respectively.

coefficient of water has been determined inside the "no man's land", through a measurement of the ice growth rate of a ~ 7 nm thick water film on a polycrystalline ice substrate (16). In this article, via extensive computer simulations of two water models and analysis of new experimental data below $T_{\rm W}$, we provide new evidence strongly supporting a microscopic two-state scenario, while running against the scenarios based on either the glass transition or the Widom line for the fragile-to-strong transition in supercooled water.

In the two-state scenario, water can be regarded as a dynamical mixture of two types of local structures (or two states), whose fraction changes with temperature and pressure, accounting for the thermodynamic anomalies of water (13, 14, 17–24). Evidence supporting the existence of two states in liquid water has been found by Raman spectroscopy (25–27), femtosecond mid-IR pump-probe spectroscopy (28), time-resolved optical Kerr effect spectroscopy (29), x-ray absorption (30) and emission spectroscopies (31). Despite the great success of two-state model for water's thermodynamic anomalies, its relevance for dynamical properties is far from clear. Recently, Singh and coworkers (32) reported a good fitting of a two-state model to water's dynamic properties. However, this work and previous two-state models for thermodynamics, were based on a phenomenological two-state description of physical quantities and lack of microscopic support: in other words, the basic two states were unidentified at a molecular level and their presence was presupposed.

With the help of a microscopic structrual descriptor ζ (18), two types of local structures (high-temperature disordered state denoted by ρ and low-temperature ordered state denoted by S hereafter) were successfully detected from a bimodal distribution of ζ, providing a solid microscopic basis for a two-state description of water (33) (Fig. S1). Typical configurations of ρ and S states are given in Figs. 1A and B, respectively. A good correlation can be found between ζ (Fig. 1C) and local density (Fig. 1D), which underlies a two-state description of water's density anomaly.

Here we also find that the molecular mobility (Fig. 1F), is correlated 'not' to ζ, but instead to its coarse-grained version $\zeta^{\rm CG}$ (Fig. 1E) (see SI Sec. II). This result is confirmed by a good correlation between $\zeta^{\rm CG}$ and mobility (Fig. S2), suggestive of a dynamic bimodality: the slow water has larger $\zeta^{\rm CG}$ than the fast one. This finding can be understood from the fact that, while the structure in a fluid is a local property, the dynamics of a water molecule is instead intrinsically coupled to that of its neighbors (nonlocal). The structural and dynamical bimodalities, linked via spatial coarse-graining, together provide a microscopic structural basis for a unified description of water's thermodynamic and dynamical anomalies.

Under the following two assumptions, (1) any pure state (either fast or slow water state) follows an Arrhenius law and (2) the lifetime of a state is shorter than the typical dynamical timescale (e.g. rotational time), a dynamical quantity X can be expressed by a generalized Arrhenius law as (13, 14)

$$X = X_0 \exp\left(\frac{E_{\rm a}^{\rho,X} + \Delta E_{\rm a}^{X} \cdot s^{\rm D}}{k_{\rm B}T}\right), \qquad [1]$$

where $E_{\rm a}^{S,X}$ and $E_{\rm a}^{\rho,X}$ are the activation energies for the slow and fast water, respectively, $\Delta E_{\rm a}^{X} = E_{\rm a}^{S,X} - E_{\rm a}^{\rho,X}$ is the activation energy difference, X_0 is the prefactor, $s^{\rm D}$ is the fraction of slow water and $k_{\rm B}$ is the Boltzmann constant. The fraction $s^{\rm D}$, following two-state behavior (Fig. S3), can be emperically described by a two-state equation (13, 14, 17, 33, 34) as follows:

$$s^{\rm D} = \frac{1}{1 + \exp\left(\frac{\Delta E^{\rm D} - T\Delta\sigma^{\rm D} + P\Delta V^{\rm D}}{k_{\rm B}T}\right)}, \qquad [2]$$

where $\Delta E^{\rm D}$, $\Delta\sigma^{\rm D}$ and $\Delta V^{\rm D}$ are fitting parameters. At ambient pressure, the term $P\Delta V^{\rm D}$ in Eq. (2) is negligible.

We note that Singh and coworkers (32) have recently proposed a different two-state model by assuming that fast water follows Vogel-Fulcher-Tammann (VFT), instead of Arrhenius behavior. This analysis is based on the presence of a critical point at low pressure ($T_c = 228.2$ K and $P_c = 0$ MPa) (35), and a divergence of the dynamics at a finite temperature ($T = 147.75$ K). This model seem inconsistent with experimental measurements that found neither a critical point (15, 36) nor divergent dynamics (5, 6, 16) at ambient pressure.

Figures 1A and B (upper panel) show water's reorientational time τ_2 (square symbols) and inverse diffusion coefficient $1/D$ (circle symbols) down to ~ 30 K below the Widom line in TIP5P and ST2 water at 0.1 MPa. The dramatic slowing down of dynamics by ~ 7 and ~ 4 orders of magnitude for TIP5P and ST2 water, respectively, can be nicely described by Eqs. (1)-(2) (solid curves). We note that the same data can also be well described by the Widom line scenario (Figs. S4 and S5). However, the two-state scenario and the Widom line scenario make very different predictions below $T_{\rm W}$.

In the Widom line scenario, water's dynamics follows a power law above $T_{\rm W}$ (in agreement with MCT) and an Arrhenius law below $T_{\rm W}$ (8, 10, 38). Although experimental measurements of diffusion (39, 40), viscosity (39, 40), and

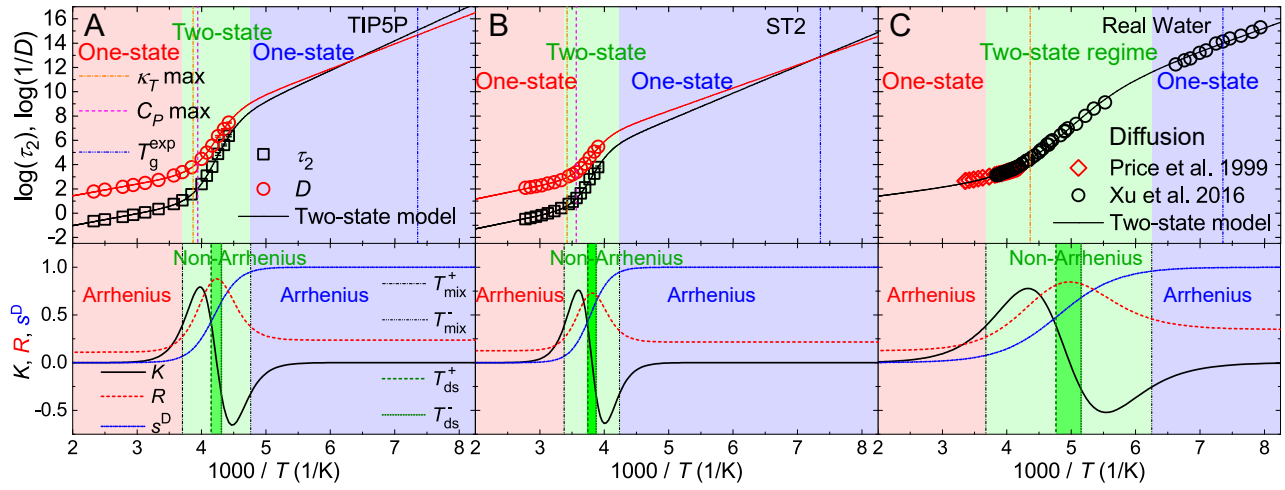

Fig. 2. Two-state scenario for the fragile-to-strong transition in TIP5P (A), ST2 (B) and real water (C). (Upper panel) The reorientational time τ_2 (in ps) and inverse diffusion coefficient $1/D$ (in $10^6 \mathrm{sm}^{-2}$) in log scale. The solid curves are fits to the two-state model. (Lower panel) The curvature K (in the units of 160 (kcal/mol)^2 for models and 40 (kcal/mol)^2 for real water), the rate R (in the units of 40 kcal/mol for models and 25 kcal/mol for real water) of $\ln(D/D_0)$, and the fraction s^{D} of slow water as a function of inverse temperature. In (A) and (B), κ_T and C_P maximum lines were taken from Ref. (10). In (C), κ_T maximum line was taken from Ref. (15), black cicle symbols from Ref. (16) and red square symbols from Ref. (37). We can see by comparing panels (A)-(C) that the width of the dynamic transition is much narrower for water models than for real water. This originates from the fact that these water models, though they capture the essential features of real water, have a much stronger tendency to form locally favoured structures than real water, as can be seen in the two-state model parameters listed in Tables S1-S3.

relaxation time (39, 41, 42) support a power-law behavior of liquid water above T_{W} at low pressure, there are at least three difficulties with this interpretation: (1) the relation between the experimental power-law divergence temperature (T_{MCT}) and T_{g}, $T_{\mathrm{MCT}} \simeq 1.6T_{\mathrm{g}}$ (40), violates the empirical rule $T_{\mathrm{MCT}} \simeq 1.2T_{\mathrm{g}}$ found in other glass formers; (2) the large difference between T_{g} and T_{W} causes unrealistic prediction of either a too long relaxation time at $T_{\mathrm{g}} = 136$ K or a too high glass transition temperature, which is more obvious ($T_{\mathrm{g}}/T_{\mathrm{m}} \simeq 0.65 \sim 0.7$) in the water models (see SI section V); (3) the Widom line scenario cannot explain the new experimental diffusion data below T_{W} (Fig. S6). On the other hand, the two-state scenario not only gives reasonable reorientational time scales (10^3 s for TIP5P and 10 s for ST2) and diffusion coefficients at T_{g}, but also provides a quantitative description of experimental diffusion data over a wide temperature range (126 K$< T <$ 298 K) (Fig. 2).

From Eqs. (1)-(2), we can define a rate R (first derivative) and a curvature K (second derivative) of $\ln \frac{X}{X_0}$ with respective to $\beta \equiv \frac{1}{k_{\mathrm{B}}T}$ by

$$R = \frac{\partial \ln \frac{X}{X_0}}{\partial \beta} = E_{\mathrm{a}}^{\rho,X} + \beta \Delta E_{\mathrm{a}}^{X} \Delta E^{\mathrm{D}} \left[\left(s^{\mathrm{D}} - \frac{1}{2} + \frac{1}{2\beta \Delta E^{\mathrm{D}}} \right)^2 - \left(\frac{1}{2} - \frac{1}{2\beta \Delta E^{\mathrm{D}}} \right)^2 \right], \quad [3]$$

$$K = \frac{\partial^2 \ln \frac{X}{X_0}}{\partial \beta^2} = 2\beta \Delta E_{\mathrm{a}}^{X} \left(\Delta E^{\mathrm{D}} \right)^2 s^{\mathrm{D}} \left(s^{\mathrm{D}} - 1 \right) \left(s^{\mathrm{D}} - \frac{1}{2} + \frac{1}{\beta \Delta E^{\mathrm{D}}} \right). \quad [4]$$

The curves of s^{D}, R and K are plotted in Figs. 2A-C (lower panels). The curvature K, as a measure of deviation from Arrhenius behavior goes to zero when $s^{\mathrm{D}} \to 0$ or $s^{\mathrm{D}} \to 1$, suggesting an Arrhenius behavior of water in the one-state regimes. At $0 < s^{\mathrm{D}} < 1$ (two-state regime), K exhibits two peaks (positive and negative), indicative of two types of non-Arrhenius behaviors (convex and concave), as shown in Fig. 2 (upper panels). Here we define the temperatures at half height of the two peaks of K by T^+_{mix}, T^+_{ds}, T^-_{ds} and T^-_{mix} from high to low temperature.

With these characteristic temperatures we define three regimes: the one-state (fast water) regime (red region) at $T > T^+_{\mathrm{mix}}$, the two-state regime (light green region) at $T^-_{\mathrm{mix}} < T < T^+_{\mathrm{mix}}$, and the one-state (slow water) regime (blue region) at $T < T^-_{\mathrm{mix}}$. Within the two-state regime we can also identify a specific band, i.e. the dynamic Schottky (DS) band (dark green region) at $T^-_{\mathrm{ds}} < T < T^+_{\mathrm{ds}}$. Equation (4) tells us that the dynamics of water should show a crossover from an Arrhenius behavior ($K \sim 0$ and constant R) in the fast-water dominant regime ($s^{\mathrm{D}} \sim 0$) to another Arrhenius behavior ($K \sim 0$ and constant R) in the slow-water dominant regime ($s^{\mathrm{D}} \sim 1$). As shown in Fig. 2C, the diffusion coefficient measured in bulk water indeed shows such crossover behavior, in agreement with measurements in confined (3, 4) and amorphous water (5, 6). The second Arrhenius behavior is usually called strong behavior, according to Angell's scheme (43).

In the narrow DS band, $s^{\mathrm{D}} \sim \frac{1}{2}$, R maximizes (Eq. (3)), and $K \to 0$ (Eq. (4)), indicative of an Arrhenius behavior inside

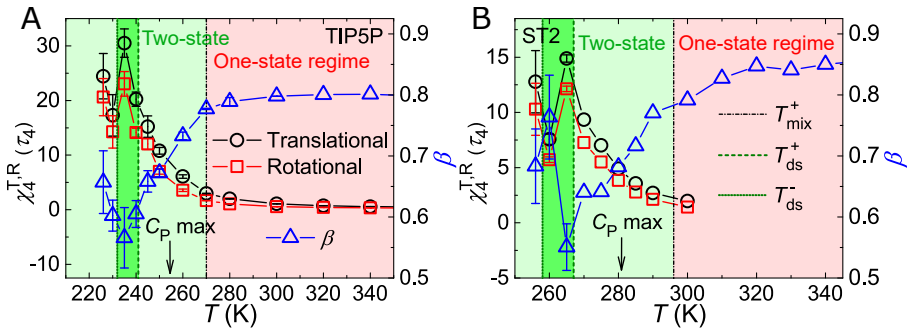

Fig. 3. Dynamic heterogeneity in TIP5P (A) and ST2 (B) water. Both translational (black circle) and rotational (red square) four-point susceptibilities $\chi_4^{\mathrm{T,R}}(\tau_4)$ maximize around $T_{s^{\mathrm{D}}=\frac{1}{2}}$ in the DS band (dark green region), providing strong evidence of the two-state behavior. The stretching parameter β (blue triangle), which is determined by fitting the stretched exponential function to the second Legendre polynomial of time correlation function of molecular dipole moment (Eqs. (S1) and (S2), also shows a minimum around $T_{s^{\mathrm{D}}=\frac{1}{2}}$ in the DS band. The locations of heat capacity maxima of the two water models are indicated by arrows.

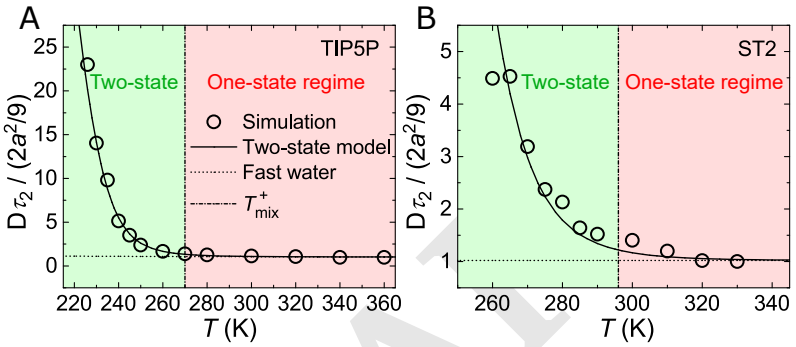

Fig. 4. Breakdown of the Stokes-Einstein-Debye relation in TIP5P (A) and ST2 (B) water. Solid and dot lines represent the two-state and individual fast-water contributions, respectively, indicating that the growth of slow water upon cooling results in the breakdown of the Stokes-Einstein-Debye relation in supercooled water. The effective hydrodynamic radius $a = 1.3$ and 1.2 Å was estimated from the high temperature data for TIP5P and ST2 water, respectively.

the two-state regime. (Fig. 2) Importantly, the DS band is located at ~ 20 K below T_{W}. The Arrhenius behavior and the maximum of R explain why the Widom line scenario predicts an apparently "strong" behavior with a too large activation energy below T_{W} (Figs. S4-S7). However, from Eqs. (3) and (4), we know that the apparent "strong" behavior in the DS band originates from the maximal rate of dynamic slowing down upon cooling, and is fundamentally different from the inherent strong behavior in the slow-water dominant regime.

We will now show that the presence of dynamic bimodality can be directly inferred from the study of dynamic heterogeneities. The four-point susceptibility $\chi_4(t)$ is a measure of the fluctuations of dynamics, i.e. dynamic heterogeneities (Eqs. (S3)-(S4)). $\chi_4(t)$ has a maximum at a dynamical timescale τ_4 (Figs. S7-S10). For normal glass-forming liquids, the maximum $\chi_4(\tau_4)$ increases monotonically as approaching the glass transition temperature T_{g}. Contrary to this glass phenomenology, for TIP5P and ST2 water both translational and rotational susceptibility $\chi_4^{\mathrm{T,R}}(\tau_4)$ maximize near $T_{s^{\mathrm{D}}=\frac{1}{2}}$ in the DS band where the system is half fast and half slow water (Fig. 3), similarly to the maximization of the thermodynamic response functions near the Widom line (10). The maximization of dynamic heterogeneity can also be seen from the behavior of the stretching parameter β (Eq. (S2)), which describes the deviation of molecular dipole reorientation from the Debye process ($\beta = 1$). Non-Debye behavior ($\beta < 1$) is usually attributed to heterogeneous dynamics. Figure 3 shows that β minimizes at $T_{s^{\mathrm{D}}=\frac{1}{2}}$, again confirming the maximization of dynamic heterogeneity in the DS band. We argue that this is a unique feature of the two-state scenario, which is known as the Schottky anomaly (18, 44). We stress that this feature cannot be explained by the scenarios based on the glass transition, where $\chi_4(\tau_4)$ should increase monotonically when approaching T_{g}, and thus in principle no $\chi_4(\tau_4)$ maximization should occur above T_{g}. Moreover, the observed maximization occurs at ~ 20 K below the Widom line, which indicates a significant difference between thermodynamic and dynamic fluctuations, in agreement with the crucial role of coarse-graining that we found in Figs. 1, S2, and S3.

It was shown that χ_4 may suffer from finite size effects in a simulation of 1000 particles, if the correlation length exceeds 6 particle size (45). Here we calculated the dynamic correlation length ξ_4 from the spatial correlation function of dynamic heterogeneity (46) (Eqs. (S5) and (S6)) in TIP5P water (Fig. S12). A maximum correlation length of ~ 6 Å or ~ 2 molecular size, was found at $T_{s^{\mathrm{D}}=\frac{1}{2}}$ (Fig. S13). This agrees with a maximal structural correlation length of ~ 4 Å at 229.2 K that was report recently by femtosecond x-ray scattering (15). This short correlation length confirms that the finite size effects, if any, should be negligible in our systems. We also performed several independent microsecond simulations to check the sample-to-sample fluctuations at low temperatures

(Table S4), which provides the error bars in Fig. 3. Clearly the maximization of χ_4 that we found in Fig. 3 is not a consequence of statistical errors.

Despite the very long simulation times (Table S4), due to the significant increase of the structural relaxation time, the lowest-temperature data still suffer from large statistical fluctuations. Nevertheless, we can see the clear increase of $\chi_4(\tau_4)$ at the lowest temperature. We speculate that this may reflect a general tendency of the dynamic susceptibility to monotonically increase upon cooling. Such behavior is known even for a system with only local dynamics, obeying the Arrhenius behavior, which may be the case for water (Eq. (1)) (47). We note that the temperature is still too far way from the glass transition temperature T_g to have glassy dynamical heterogeneity. We will study this problem in more detail in the future.

In normal glass-forming liquids, rotational motion decouples from translational diffusion below $\sim 1.2T_g$ (48), which is known as the breakdown of the Stokes-Einstein and Stokes-Einstein-Debye relations ($D\tau_2 = 2a^2/9$, where a is an effective hydrodynamic radius), and which is believed to be a consequence of glassy dynamic heterogeneity. However, as shown in Fig. 4, the breakdown happens much earlier ($\sim 2T_g$) than $1.2T_g$ for TIP5P and ST2 water, which along with the abnormal high MCT temperature $T_{MCT} \simeq 1.6T_g$ (40) questions the glass transition scenario. Here we show that this anomalous behavior can also be naturally explained by the two-state scenario. Applied to diffusive and rotational motions, Eq. (1) gives a new explanation to the Stokes-Einstein-Debye relation by

$$\begin{aligned} D\tau_2 &= D_0\tau_0 \exp\left[\frac{E_a^{\rho,\tau} - E_a^{\rho,D}}{k_B T}\right] \cdot \exp\left[\frac{\Delta E_a^{\tau} - \Delta E_a^{D}}{k_B T} \cdot s^D\right] \\ &\approx D_0\tau_0 \exp\left[\frac{\Delta E_a^{\tau} - \Delta E_a^{D}}{k_B T} \cdot s^D\right]. \end{aligned} \quad [5]$$

The second equation above is valid only if the activation energies for rotation and diffusion equal in the fast-water dominant state ($E_a^{\rho,\tau} \approx E_a^{\rho,D}$), i.e. rotation is coupled to diffusion. This is true, since the Stokes-Einstein-Debye relation holds at high temperature, where $s^D \sim 0$. This is also confirmed by our fitting result (Tables S2 and S3). In the fast-water dominant state ($T > T_{mix}^{+}$, red), translational motion couples to reorientation. However, the activation energy for reorientation becomes considerably higher than translation in the slow-water dominant state (Tables S2 and S3), so the reorientation will slow down much faster than translation upon cooling, which leads to the breakdown of the Stokes-Einstein-Debye relation (see Eq. (5)). It can be seen clearly in Fig. 4 that the fast-water dominant state follows the Stokes-Einstein-Debye relation quite well, and the decoupling behavior can be perfectly described by the prediction of the two-state model (Eq. (5)), indicating that the anomalous breakdown mainly comes from the growth of the slow-water dominant state upon cooling, and not from glassiness.

Finally, we compare the temperature dependence of water's diffusion coefficient with a typical fragile liquid (*o*-Terphenyl) and a strong liquid (SiO_2) in Fig. 5. The two-state model quantitatively describes water's fragile-to-strong transition as a crossover from one Arrhenius to another Arrhenius behavior. Water's dynamical slowing down starts much further above T_g than the case of normal fragile liquid, *o*-Terphenyl.

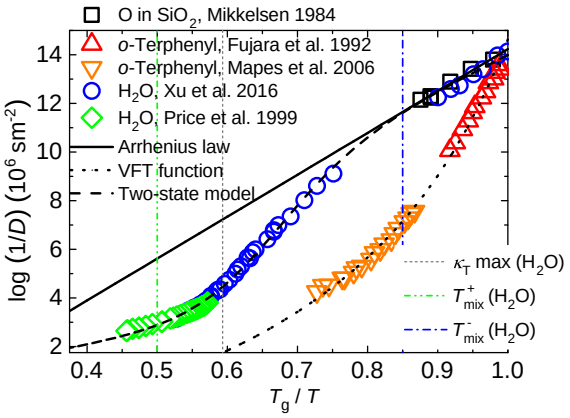

Fig. 5. Angell plot of experimental liquid diffusivities. Water's diffusion slows down rapidly when entering the two-state mixture regime ($T_{mix}^{+} > T > T_{mix}^{-}$) from high temperature, showing its apparent fragile nature far above T_g than normal fragile liquid, *o*-Terphenyl. Near the Widom line (κ_T max), water's diffusion apparently follows the Arrhenius law (curvature $k \simeq 0$), but deviates from the typical strong behavior of SiO_2. Water shows its inherent strong nature like SiO_2 when leaving the two-state mixture regime and entering the slow-water dominant regime ($T < T_{mix}^{-}$). κ_T maximum line of water was taken from Ref. (15), oxygen diffusivity in SiO_2 from Ref. (49), *o*-Terphenyl diffusivity from Refs. (50) and (51), water diffusivity from Refs. (16) and (37).

This feature, along with the abnormal high MCT temperature $T_{MCT} \simeq 1.6T_g$, and the early breakdown of the Stokes-Einstein-Debye relation at $\sim 2T_g$, strongly suggests an apparently fragile behavior of water essentially different from that of normal fragile glass-formers. The former comes from the formation of two states (fast and slow water) below $T_{mix}^{+} \simeq T_M \simeq 2T_g$, while the latter originates from the glass transition at T_g. These features, together with the failure of power law at high pressure (41) and the maximization of dynamic heterogeneity, provide strong evidence for the two-state scenario.

The two-state scenario predicts a novel DS band, where dynamic heterogeneity maximizes and the dynamics apparently obeys the Arrhenius law. This feature naturally explains the observations of a "strong" behavior of water just below the Widom line. However, here we have shown that this apparent strong behavior, as a two-state feature, is fundamentally different from water's inherent strong nature near T_g, as can be seen from its large deviation from the typical strong behavior of SiO_2 at the Widom line (κ_T maximum line) in Fig. 5. We also note that the calculated maximal dynamic correlation length of ~ 6 Å together with a maximal structural correlation length of ~ 4 Å reported recently by femtosecond x-ray scattering (15), supports the two-state scenario based on local structural ordering, but runs against scenarios relying on an extended length scale from either a glass transition or a critical point, at least at ambient pressure.

Water-like dynamic anomalies in the form of fragile-to strong transitions, which were pioneered by Angell and his coworkers (1, 2, 52), have been seen in many glass-formers such as tetrahedral liquids (see, e.g., Refs. (53, 54)) and metallic liquids (see, e.g., Ref. (55)), and they are also located far above the glass transition temperature, as in the case of water. On noting that many of these liquids have a tendency to form locally favoured structures in the form of tetrahedral or

icosahedral structures, we argue that these behaviors may also be caused by a similar two-state feature originating from local structural ordering (34), instead of glassiness. We hope that our work will initiate further researches along this direction.

ACKNOWLEDGMENTS. We thank Y. Xu and his colleagues (the authors of Ref. (16)) for providing us the raw data of the diffusion coefficient. This study was partly supported by Scientific Research (S) and Specially Promoted Research (KAKENHI Grants No. 21224011 and No. 25000002 respectively) from the Japan Society for the Promotion of Science (JSPS). JR acknowledges support from the ERC Grant DLV-759187 and the Royal Society University Research Fellowship.

1. CA Angell. Water II is a" strong" liquid. *J. Phys. Chem.*, 97(24):6339–6341, 1993.
2. Kaori Ito, Cornelius T Moynihan, and C Austen Angell. Thermodynamic determination of fragility in liquids and a fragile-to-strong liquid transition in water. *Nature*, 398(6727):492–495, 1999.
3. Francesco Mallamace, Carmelo Corsaro, Piero Baglioni, Emiliano Fratini, and Sow-Hsin Chen. The dynamical crossover phenomenon in bulk water, confined water and protein hydration water. *J. Phys. Condens. Matter*, 24(6):064103, 2012.
4. Silvina Cerveny, Francesco Mallamace, Jan Swenson, Michael Vogel, and Limei Xu. Confined water as model of supercooled water. *Chem. Rev.*, 116:7608–7625, 2016.
5. Catalin Gainaru, Alexander L Agapov, Violeta Fuentes-Landete, Katrin Amann-Winkel, Helge Nelson, Karsten W Köster, Alexander I Kolesnikov, Vladimir N Novikov, Ranko Richert, Roland Böhmer, Thomas Loerting, and Alexei P. Sokolov. Anomalously large isotope effect in the glass transition of water. *Proc. Natl. Acad. Sci. U. S. A.*, 111(49):17402–17407, 2014.
6. Thomas Loerting, Violeta Fuentes-Landete, Philip H Handle, Markus Seidl, Katrin Amann-Winkel, Catalin Gainaru, and Roland Böhmer. The glass transition in high-density amorphous ice. *J. Non-Cryst. Solids*, 407:423–430, 2015.
7. CA Angell. Liquid fragility and the glass transition in water and aqueous solutions. *Chem. Rev.*, 102(8):2627–2650, 2002.
8. M De Marzio, G Camisasca, M Rovere, and P Gallo. Mode coupling theory and fragile to strong transition in supercooled tip4p/2005 water. *J. Chem. Phys.*, 144(7):074503, 2016.
9. G. P. Johari, Andreas Hallbrucker, and Erwin Mayer. The glass-liquid transition of hyperquenched water. *Nature*, 330:552–553, 1987. .
10. Limei Xu, Pradeep Kumar, S. V. Buldyrev, S. H. Chen, P. H. Poole, F. Sciortino, and H. E. Stanley. Relation between the Widom line and the dynamic crossover in systems with a liquid-liquid phase transition. *Proc. Natl. Acad. Sci. U. S. A.*, 102(46):16558–16562, 2005. .
11. Peter H. Poole, Francesco Sciortino, Ulrich Essmann, and H. Eugene Stanley. Phase behavior of metastable water. *Nature*, 360(6402):324–328, 1992.
12. Jeremy C. Palmer, Fausto Martelli, Yang Liu, Roberto Car, Athanassios Z. Panagiotopoulos, and Pablo G. Debenedetti. Metastable liquid-liquid transition in a molecular model of water. *Nature*, 510(7505):385–388, 2014.
13. Hajime Tanaka. Simple physical model of liquid water. *J. Chem. Phys.*, 112:799–809, 2000. .
14. Hajime Tanaka. A new scenario of the apparent fragile-to-strong transition in tetrahedral liquids: water as an example. *J. Phys.: Condens. Matter*, 15:L703–L711, 2003. .
15. Kyung Hwan Kim, Alexander Späh, Harshad Pathak, Fivos Perakis, Daniel Mariedahl, Katrin Amann-Winkel, Jonas A Sellberg, Jae Hyuk Lee, Sangsoo Kim, Jaehyun Park, et al. Maxima in the thermodynamic response and correlation functions of deeply supercooled water. *Science*, 358(6370):1589–1593, 2017.
16. Yuntao Xu, Nikolay G Petrik, R Scott Smith, Bruce D Kay, and Greg A Kimmel. Growth rate of crystalline ice and the diffusivity of supercooled water from 126 to 262 k. *Proc. Natl. Acad. Sci. U. S. A.*, 113(52):14921–14925, 2016.
17. Hajime Tanaka. Thermodynamic anomaly and polyamorphism of water. *EPL*, 50:340–346, 2000. .
18. John Russo and Hajime Tanaka. Understanding water's anomalies with locally favoured structures. *Nat. Commun.*, 5:3556, 2014. .
19. V. Holten and M. A. Anisimov. Entropy-driven liquid-liquid separation in supercooled water. *Sci. Rep.*, 2:713, 2012. .
20. Vincent Holten, David T Limmer, Valeria Molinero, and Mikhail A. Anisimov. Nature of the anomalies in the supercooled liquid state of the mw model of water. *J. Chem. Phys.*, 138(17):174501, 2013.
21. Vincent Holten, Jeremy C. Palmer, Peter H. Poole, Pablo G. Debenedetti, and Mikhail A. Anisimov. Two-state thermodynamics of the ST2 model for supercooled water. *J. Chem. Phys.*, 140(10):104502, 2014. .
22. Rakesh S. Singh, John W. Biddle, Pablo G. Debenedetti, and Mikhail A. Anisimov. Two-state thermodynamics and the possibility of a liquid-liquid phase transition in supercooled tip4p/2005 water. *J. Chem. Phys.*, 144(14):144504, 2016.
23. John W. Biddle, Rakesh S. Singh, Evan M. Sparano, Francesco Ricci, Miguel A. González, Chantal Valeriani, JoséL. F. Abascal, Pablo G. Debenedetti, Mikhail A. Anisimov, and Frédéric Caupin. Two-structure thermodynamics for the tip4p/2005 model of water covering supercooled and deeply stretched regions. *J. Chem. Phys.*, 146(3):034502, 2017. .
24. Mikhail A Anisimov, Michal Duška, Frédéric Caupin, Lauren E Amrhein, Amanda Rosenbaum, and Richard J Sadus. Thermodynamics of fluid polyamorphism. *Phys. Rev. X*, 8(1):011004, 2018.
25. GE Walrafen. Raman spectral studies of water structure. *J. Chem. Phys.*, 40(11):3249–3256, 1964.
26. GE Walrafen. Raman spectral studies of the effects of temperature on water structure. *J. Chem. Phys.*, 47(1):114–126, 1967.
27. GE Walrafen, MR Fisher, MS Hokmabadi, and W-H Yang. Temperature dependence of the low-and high-frequency raman scattering from liquid water. *J. Chem. Phys.*, 85(12):6970–6982, 1986.
28. S Woutersen, U Emmerichs, and HJ Bakker. Femtosecond mid-ir pump-probe spectroscopy of liquid water: Evidence for a two-component structure. *Science*, 278(5338):658–660, 1997.
29. A. Taschin, P. Bartolini, R. Eramo, R. Righini, and R. Torre. Evidence of two distinct local structures of water from ambient to supercooled conditions. *Nat. Commmun.*, 4:2401, 2013.
30. Jonas A Sellberg, Sarp Kaya, Vegard H Segtnan, Chen Chen, Tolek Tyliszczak, Hirohito Ogasawara, Dennis Nordlund, Lars GM Pettersson, and Anders Nilsson. Comparison of x-ray absorption spectra between water and ice: New ice data with low pre-edge absorption cross-section. *J. Chem. Phys.*, 141(3):034507, 2014.
31. Congcong Huang, K Thor Wikfeldt, Takashi Tokushima, Dennis Nordlund, Yoshi Harada, Uwe Bergmann, Marc Niebuhr, TM Weiss, Yoshi Horikawa, Mikael Leetmaa, et al. The inhomogeneous structure of water at ambient conditions. *Proc. Natl. Acad. Sci. U.S.A.*, 106(36):15214–15218, 2009.
32. Lokendra P. Singh, Bruno Issenmann, and Frédéric Caupin. Pressure dependence of viscosity in supercooled water and a unified approach for thermodynamic and dynamic anomalies of water. *Proc. Natl. Acad. Sci. U. S. A.*, 114(17):4312–4317, 2017. . URL http://www.pnas.org/content/114/17/4312.abstract.
33. Rui Shi and Hajime Tanaka. Microscopic structural descriptor of liquid water. *J. Chem. Phys.*, 148:124503, 2018. .
34. Rui Shi and Hajime Tanaka. Impact of local symmetry breaking on the physical properties of tetrahedral liquids. *Proc. Natl. Acad. Sci. U. S. A.*, 115(9):1980–1985, 2018. .
35. Vincent Holten, Jan V. Sengers, and Mikhail A. Anisimov. Equation of state for supercooled water at pressures up to 400 mpa. *J. Phys. Chem. Ref. Data*, 43(4):043101, 2014.
36. JA Sellberg, C Huang, TA McQueen, ND Loh, H Laksmono, D Schlesinger, RG Sierra, D Nordlund, CY Hampton, D Starodub, DP DePonte, M Beye, C Chen, AV Martin, A Barty, KT Wikfeldt, TM Weiss, C Caronna, J Feldkamp, LB Skinner, MM Seibert, M Messerschmidt, GJ Williams, S Boutet, LGM Pettersson, MJ Bogan, and A Nilsson. Ultrafast x-ray probing of water structure below the homogeneous ice nucleation temperature. *Nature*, 510(7505):381–384, 2014.
37. William S. Price, Hiroyuki Ide, and Yoji Arata. Self-diffusion of supercooled water to 238 k using pgse nmr diffusion measurements. *J. Phys. Chem. A*, 103(4):448–450, 1999.
38. M De Marzio, G Camisasca, M Rovere, and P Gallo. Microscopic origin of the fragile to strong crossover in supercooled water: The role of activated processes. *J. Chem. Phys.*, 146(8):084502, 2017.
39. R. J. Speedy and C. A. Angell. Isothermal compressibility of supercooled water and evidence for a thermodynamic singularity at -45° C. *J. Chem. Phys.*, 65:851, 1976. .
40. Amine Dehaoui, Bruno Issenmann, and Frédéric Caupin. Viscosity of deeply supercooled water and its coupling to molecular diffusion. *Proc. Natl. Acad. Sci. U. S. A.*, 112(39):12020–12025, sep 2015. . URL http://www.pnas.org/content/112/39/12020.abstract.
41. E. W. Lang and H. D. Lüdemann. High pressure O^{17} longitudinal relaxation time studies in supercooled H_2O and D_2O. *Ber. Bunsenges. Phys. Chem.*, 85(7):603–611, jul 1981. . URL http://dx.doi.org/10.1002/bbpc.19810850716.
42. Renato Torre, Paolo Bartolini, and Roberto Righini. Structural relaxation in supercooled water by time-resolved spectroscopy. *Nature*, 428(6980):296, 2004.
43. C Austen Angell. Formation of glasses from liquids and biopolymers. *Science*, 267(5206):1924–1935, 1995.
44. H. Tanaka. Bond orientational order in liquids: Towards a unified description of water-like anomalies, liquid-liquid transition, glass transition, and crystallization. *Eur. Phys. J E*, 35:113, 2012.
45. Smarajit Karmakar, Chandan Dasgupta, and Srikanth Sastry. Growing length and time scales in glass-forming liquids. *Proc. Natl. Acad. Sci. U. S. A.*, 106(10):3675–3679, 2009.
46. N Lačević, Francis W Starr, TB Schrøder, VN Novikov, and SC Glotzer. Growing correlation length on cooling below the onset of caging in a simulated glass-forming liquid. *Phys. Rev. E*, 66(3):030101, 2002.
47. Ludovic Berthier, Giulio Biroli, J-P Bouchaud, Walter Kob, Kunimasa Miyazaki, and DR Reichman. Spontaneous and induced dynamic fluctuations in glass formers. i. general results and dependence on ensemble and dynamics. *J. Chem. Phys.*, 126(18):184503, 2007.
48. Pablo G. Debenedetti. Supercooled and glassy water. *J. Phys.: Condens. Matter*, 15:1669–1726, 2003. .
49. JC Mikkelsen Jr. Self-diffusivity of network oxygen in vitreous SiO2. *Appl. Phys. Lett.*, 45(11):1187–1189, 1984.
50. F Fujara, B Geil, H Sillescu, and G Fleischer. Translational and rotational diffusion in supercooled orthoterphenyl close to the glass transition. *Z. Phys. B - Condensed Matter*, 88(2):195–204, 1992.
51. Marie K Mapes, Stephen F Swallen, and MD Ediger. Self-diffusion of supercooled o-terphenyl near the glass transition temperature. *J. Phys. Chem. B*, 110(1):507–511, 2006.
52. C. Austen Angell. Insights into phases of liquid water from study of its unusual glass-forming properties. *Science*, 319:582–587, 2008.
53. CA Angell, RD Bressel, M Hemmati, EJ Sare, and JC Tucker. Water and its anomalies in perspective: tetrahedral liquids with and without liquid–liquid phase transitions. invited lecture. *Phys. Chem. Chem. Phys.*, 2(8):1559–1566, 2000.
54. Ivan Saika-Voivod, Peter H. Poole, and Francesco Sciortino. Fragile-to-strong transition and polyamorphism in the energy landscape of liquid silica. *Nature*, 412(6846):514–517, 2001.
55. Chunzhi Zhang, Lina Hu, Yuanzheng Yue, and John C Mauro. Fragile-to-strong transition in metallic glass-forming liquids. *J. Chem. Phys.*, 133(1):014508, 2010.